Functionalized Sol–Gel Coatings for Optical Applications

ANNE-LAURE PÉNARD, THIERRY GACOIN, AND JEAN-PIERRE BOILOT*

Groupe de Chimie du Solide, Laboratoire de Physique de la Matière Condensée, CNRS, École Polytechnique, 91128 Palaiseau cedex, France

Received November 2, 2006

ABSTRACT

Sol–gel processing is well-known to be a powerful technique for designing materials for optical applications. Here, some recent applications of functionalized sol–gel coatings in optics are briefly reviewed. Lanthanide-doped oxide nanocrystals form a new promising class of nanophosphors allowing the easy sol–gel preparation of transparent and luminescent films for the development of light-emitting devices. Recent experiments on organized mesoporous films show their potential applications in optics, such as stable low-index layers in interferential antireflective devices or as silica binders in TiO_2-photocatalytic devices.

Introduction

It is now well-known that the mild synthesis conditions offered by the sol–gel process allow for the incorporation of optically active organic molecules into the glassy matrix to form doped gels with specific optical properties. A variety of shapes, including thin films and monoliths, can be prepared, exhibiting good optical properties (transmission in visible range) and mechanical strength (easy machining) required for optical properties.[1] Numerous silica and siloxane-based hybrid organic–inorganic materials, mainly as coatings, have been developed in the past years, showing emission (solid-state dye lasers, electroluminescent devices), photochromism (optical switching, information storage), optical nonlinearity (second-order NLO, hole-burning) and sensing properties.[2] However, a serious limitation for applications of these systems is generally the rapid photobleaching of the optically active organic molecules, which drastically limits their lifetime.

The recent development of both optically active entities, such as inorganic nanoparticles or clusters, that are more photostable than organic dyes and transparent mesoporous silica matrices prepared by reacting alkoxide precursors in the presence of templates working at the nanometer scale (amphiphilic molecules or macromolecules) offers new possibilities for the use of sol–gel processing in industrial applications.

The following Account focuses on three areas of our recent work on functionalized sol–gel coatings for optical applications: (1) luminescent and transparent films for light emission, (2) mesoporous silica films as low-index layers in interferential antireflective devices, and (3) mesoporous silica films as binders of TiO_2 nanoparticles in photocatalytic devices.

Luminescent and Transparent Films for Light Emission

Luminescent materials, also called phosphors, can be found in a large range of everyday applications such as cathode ray tubes, projection televisions, fluorescent tubes, or X-ray detectors. Considerable research activity is being carried out to improve the chemical stability and to adapt the materials chemistry to the production technology of the respective application. Classical doped solid-state materials are increasingly giving way to new material classes such as organic phosphors, composites, and nanostructured films. For example, concerning white light generation, work on white organic light-emitting diodes (WOLEDs) has led to the production of high-efficiency electrophosphorescent devices, and the first WOLEDs for general lighting are expected to be commercialized in the next years.[3] Encapsulation of phosphors or semiconductor nanocrystals in a GaN layer has also contributed to the production of white inorganic LEDs.[4]

Thin phosphor films have been prepared by a variety of deposition techniques such as chemical vapor deposition (CVD),[5] spray pyrolysis,[6] pulsed laser deposition,[7] or laser ablation.[8] These techniques are often difficult to control for complex oxide matrices or doping compositions, so the liquid route seems to be more appropriate to produce transparent films, for instance, by dispersion of light emitters in polymers or sol–gel silica matrices. Different luminescent coatings have already been obtained by sol–gel processing from alkoxide precursors[9,10] or from inorganic salts, using the Pechini method.[11,12] However, the production of dense and well-crystallized layers generally requires a thermal treatment (>800 °C), which is not compatible with the thermal stability of industrial substrates (glasses and plastics).

An alternative way to develop white emitting devices consists of the dispersion of nanophosphors, that is, luminescent nanocrystals, in transparent polymer or sol–gel matrices.[13,14] In a first step, this requires routes to synthesize nanophosphors as perfectly individualized and crystallized particles. The development of colloidal syntheses to prepare size-controlled, monodisperse, and bright nanoparticles has been largely developed in the last years, especially for semiconducting quantum dots.[15] Lanthanide-doped insulator oxides constitute an impor-

Anne-Laure Pénard has achieved her Ph.D. in ceramic materials science in the laboratory of science of ceramic processes and surface treatments (Limoges, France). She is now working on luminescent films as a postdoctoral researcher in the Solid State Chemistry group.

Thierry Gacoin is a CNRS permanent researcher (Chargé de Recherches) in the Solid State Chemistry Group of Prof. Jean-Pierre Boilot. His research concerns soft chemistry routes to nanostructured materials, mainly for applications in the field of optics.

Jean-Pierre Boilot is Associate Professor of Chemistry at the Ecole Polytechnique (France). His research group pursues interests in the physics of sol–gel polymerization, the synthesis and optical properties of molecularly designed solids such as organic–inorganic hybrid materials, oxide and semiconductor nanoparticles, and mesoporous organized oxide films.

10.1021/ar600025j CCC: $37.00
Published on Web 03/02/2007

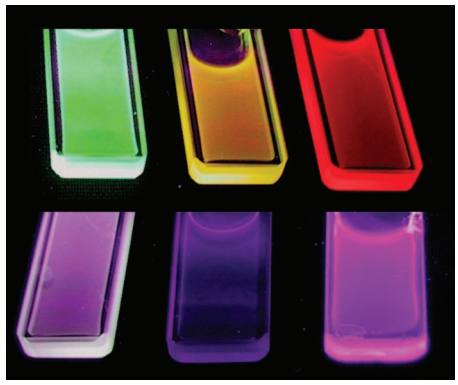

FIGURE 1. Lanthanide phosphate aqueous colloids under UV light excitation: top, [(Ce,Tb)PO_4·xH_2O/$LaPO_4$·xH_2O]/SiO_2 green and YVO_4:Eu/SiO_2 red colloids; bottom, [$CePO_4$·xH_2O/$LaPO_4$·xH_2O]/SiO_2 blue colloid. Yellow, pink, or white colloidal suspensions can be obtained by mixing the appropriate amounts of the three primary colors.

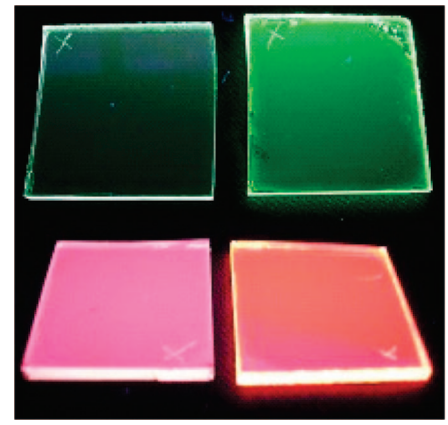

FIGURE 2. Transparent spin-coated sol–gel films under UV light excitation: top, green luminescence provided from $LaPO_4$:Ce,Tb nanocrystals in transparent films, monolayer (left) and five layers (right); bottom, red luminescence provided from YVO_4:Eu nanocrystals in transparent films before (left) and after (right) heating treatment at 450 °C for 1 h.

tant other class of nanophosphors for which different types of liquid-phase syntheses have led to the production of colloidal suspensions.[16] For example, our group developed the synthesis of lanthanide vanadate (YVO_4:Ln) and phosphate ($LaPO_4$:Ln) nanoparticles as well-dispersed and highly concentrated colloids by a simple aqueous route using competition between precipitation and complexation reactions.[17] A core–shell strategy was also reported to improve the chemical stability and the brightness of the colloidal particles, using the growth of $LaPO_4$·xH_2O and SiO_2 protective layers.[18] Under UV excitation, the three primary colors are furnished by YVO_4:Eu, $LaPO_4$:Ce·$0.7H_2O$ and $LaPO_4$:CeTb·$0.7H_2O$ aqueous colloids, which emit red, blue-violet, and green light, respectively, under UV excitation. It is thus possible to screen a large wavelength range for light emission by changing the nature of the lanthanide doping ion in yttrium vanadate and lanthanum phosphate matrices (Figure 1).[19]

The preparation of stable colloids makes possible the second key step, which is the elaboration of transparent luminescent films from a dispersion of nanophosphors in a sol, which can either be constituted of organic or inorganic polymerizable species.[20,21] The silica-type sol–gel chemistry enables a fine control of the chemical and physical properties of the matrix in which the nanophosphors are dispersed and is thus an easy way to obtain transparent and luminescent thin films by spin- or dip-coating. For example, in a preliminary study, YVO_4:Eu particles were coated with 3-(methacryloxy)propyltrimethoxysilane (TPM), and the alcoholic sol was spin-coated on various substrates leading to perfectly trans parent and highly red luminescent films of about 100 nm in thickness.[22] In spite of the high quality of these films, the complex functionalization and the use of alcoholic solvents are significant drawbacks for an industrial application. A simpler route consists in a mixing of aqueous luminescent colloidal suspensions with an inorganic binder that will ensure good mechanical properties of the film and preserve the good dispersion state of the particles. Thin films of YVO_4:Eu and $LaPO_4$:Ce,Tb, emitting in the red and green, respectively, after ultraviolet (UV) excitation, were obtained using tetramethylammonium polysilicate (Si-TMA) as inorganic binder. The thickness of the film varies between 100 and 800 nm depending on the initial concentration of the colloidal suspension, the amount of binder introduced, and the viscosity. In order to improve the brightness while keeping the transparency, it is possible either to achieve multilayers or to use thermal treatments (Figure 2). Concerning yttrium vanadate red films, a heating process for 1 h at 450 °C improves the luminescence by a factor 2.5, as a consequence of the loss of OH and organic groups, which are well-known to quench the luminescence of lanthanide ions.[23] For $LaPO_4$:Ce,Tb green films, special attention has to be paid to thermal treatments avoiding the oxidation of Ce^{3+}-doped particles both by the use of a protective shell of $LaPO_4$–xH_2O and by controlling the sintering atmosphere.[18] Although the preparation of efficient blue films remains a challenge, this simple sol–gel route should lead in a next future to the development of white-light-emitting devices either by successive depositions of three layers containing blue-, red-, and green-emitting particles, respectively, or by preparing only a single film containing a mixture of the three kinds of dispersed particles. The brightness of the deposited films could be also optimized using rapid thermal annealing treatments under different atmospheres.

Cetyltrimethylammonium Bromide (CTAB)-Templated Mesoporous Films as Low Refractive Index Layers

Many applications require an increase of the transmittance or a reduction of unwanted surface reflection of transparent materials. Examples for the former case are cover glazing for solar collectors and solar cells and wind screens for cars. Examples for the latter are cathodic ray tubes or shop windows. The usual technique to accomplish this is to apply a thin transparent film on the glass surface. This antireflection (AR) treatment can be

described within the Fresnel formalism and effective medium theories. It follows that the index of refraction of the film should be the square root of that of the substrate for optimum AR effect. For example, production of an antireflective effect at an air/glass interface at a wavelength of 500 nm requires a film with an index equal to 1.22 and a thickness of 103 nm. A common way of achieving this is to work with a porous structure.[24]

Better results can be obtained by using two thin layers instead of one. In this case, the four independent parameters (indexes and thicknesses) are chosen to yield a reflectance value near zero at two separate wavelengths so that the reflectance can be minimized over a wavelength range, which, for example, can extend over most of the visible spectrum.

Compared with more traditional coating techniques (CVD, sputtering), the potential of sol–gel-derived AR coatings has been clearly shown because the sol–gel thin film process permits independent tailoring of both chemical composition and microstructure of the deposited films.[24,26] For example, open structures can be developed in sol–gel layers obtained by the deposition of silica in colloidal state.[27]

Because of their high porosity, organized mesoporous sol–gel films have been proposed as low refractive index layers (at optical frequencies) and as low-κ dielectrics (at microelectronic frequencies, typically 1 MHz).[28,29] Mesostructured silica films are generally synthesized from a mixture containing the classic cetyltrimethylammonium bromide (CTAB) or chloride (CTAC) surfactant and a silica sol prepared by acidic hydrolysis of an ethanolic solution of alkoxysilanes, such as the tetraethoxysilane (TEOS).[28] After spin- or dip-coating deposition, the rapid removal of solvents allows both the micellar organization and its stabilization by gelation of a percolative silica network constituting the wall structure. The organized mesoporous silica films are then obtained after subsequent removal of the organic template either by calcination for glass substrates or by washing with acetone for plastic substrates. Bruinsma et al. have studied the variation of the refractive index at 500 nm as a function of CTAC/TEOS ratio.[29] Films were prepared with a pore fraction of 64% and an index of 1.16. Similar values were also obtained by Balkenende et al. using CTAB-templated hybrid films prepared by co-condensation of TEOS with methyltrimethoxysilane (MTES).[30] They showed that the presence of hydrophobic organosilane precursors, such as MTES, can both improve the stability of the index by limiting the absorption of water in the porous structure and also drastically reduce the structural organization of mesopores in films by perturbing the structure of silica clusters.

Here the potentiality of the different mesostructures observed in spin-coated CTAB-templated silica films as low index layers for AR applications are examined. A major problem is the high porosity of these films leading to a rapid introduction of contaminants from the atmosphere (water and organic molecules) implying drastic damage to the dielectric properties. The low index can be significantly stabilized in organic–inorganic hybrid mesoporous films, opening the way to their use for AR applications.

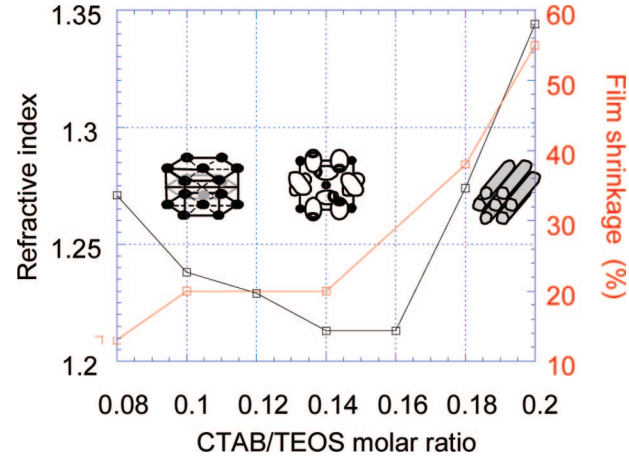

FIGURE 3. Evolution of the refractive index and of the film shrinkage as a function of the CTAB/TEOS starting ratio for CTAB-templated silica films heated at 450 °C and exhibiting different structures (successively, H3D, C, and H2D by increasing the CTAB/TEOS ratio).

As the CTAB/Si ratio increases in the initial solution, three micellar structures have been observed that are able to give highly organized mesoporous silica films:[28] a 3D hexagonal structure (H3D) formed of a dense packing of spherical micelles, a cubic structure (C) constituted of ellipsoidal micelles, and a 2D-hexagonal structure (H2D) constituted of cylindrical micelles. The amount of surfactant used for the synthesis of the films is a parameter that determines the final volume fraction of the pores and thus should be a means of controlling the refractive index of the films. Figure 3 shows the evolution of the refractive index measured at 633 nm on calcined films (450 °C) by spectroscopic ellipsometry as a function of the starting CTAB/Si ratio. As expected the refractive index starts to decrease for increasing amounts of CTAB but increases again for higher CTAB/Si ratios. Indeed, as shown by the shrinkage of films, the 2D-hexagonal mesoporous structure collapses during calcination, probably because its walls are too thin to resist excessive condensation between silanol groups. Mesoporous films with C and H3D structures present low index values (1.21–1.23), but H3D films are only considered in the following because they present the most robust structure and the most precisely defined structure (Figure 4A) since the C-films are not entirely textured.[31]

The porosity of these H3D films was rigorously characterized by ellipsometric porosimetry coupled with infrared ellipsometry (Figure 4B).[32] The total porosity, as deduced from the refractive index in the visible range and the value of the silica skeleton (1.490), reaches 55%. The mesopores (60% of the porosity) are connected to each other and to the ambient atmosphere through the micropores (40% of the porosity). The porosity of the films is entirely open to the ambient atmosphere (Figure 4C). Furthermore, the silica walls contain a great amount of polar silanol groups, which can interact with all kinds of molecules from the ambient atmosphere, even after a thermal treatment at 450 °C. As shown by infrared

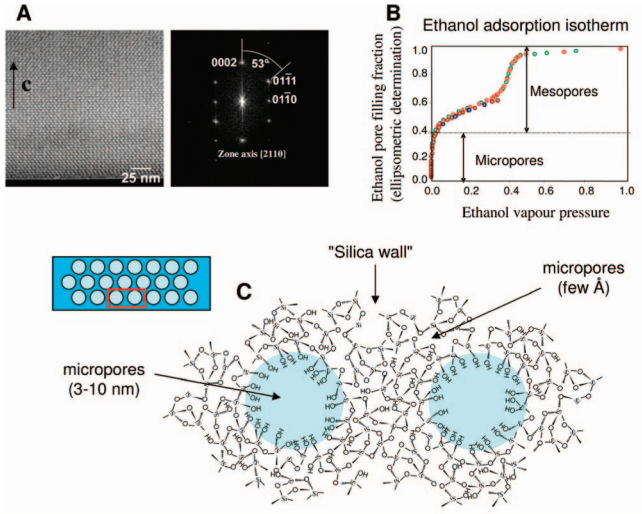

FIGURE 4. Structural characterization of the 3D-hexagonal films: (A) transverse HRTEM image and corresponding power spectrum showing that the film is perfectly organized through all the thickness with the *c* axis perpendicular to the substrate; (B) ethanol adsorption–desorption isotherms at 25 °C showing the presence of micropores (22% of the total volume) and mesopores (33% of the total volume); (C) schematization of the porosity distribution in the film.

spectroscopy studies of calcined 3D-hexagonal films left in ambient air for several months, isolated silanol groups become rapidly bonded to water molecules or other silanol groups.[32] The introduction of water from ambient humidity leads to a partial hydrolysis of siloxane bridges, preferably on the most constrained bonds. After about 10 days, organic pollutants are also present into the films. The direct consequence of this contamination is a significant increase of the refractive index of the films (already noticeable within a few hours), from 1.23 to 1.41 (Figure 5A).

Silanol groups bound on the surface of pores have to be eliminated in order to stabilize the optical properties of the films. A first strategy to solve this problem consists in a postgrafting process where Si–OH bonds are replaced by nonhydrolyzable and nonhydrophilic Si–O–Si–$(CH_3)_3$ bonds using 1,1,1,3,3,3-hexamethyldisilazane (HMDS) as reactive agent ($2Si–OH + HN–(Si(CH_3)_3)_2 \rightarrow 2Si–O–Si–(CH_3)_3 + NH_3$). A second strategy consists of the preparation of well-organized MTEOS/TEOS organosilica films by an original route recently proposed.[33] In this process, the preparation of the deposited sol is composed of two steps. Highly reactive silica clusters are prepared by hydrolysis–condensation of TEOS as in the preparation of pure silica films. Just before the sol deposition, MTES monomers are added into the aged silica sol. In this case, in contrast with a simple TEOS–MTEOS co-condensation, the reactivity of the silica clusters is not significantly perturbed when adding partially hydrolyzed MTEOS monomers. Consequently, silica gelation can take place during the fast evaporation process and stabilized well-organized H3D MTEOS/TEOS films up to 50% MTEOS. These films can be also postgrafted by HMDS to suppress the remaining silanol groups, leading to HMDS–MTES/TEOS films.

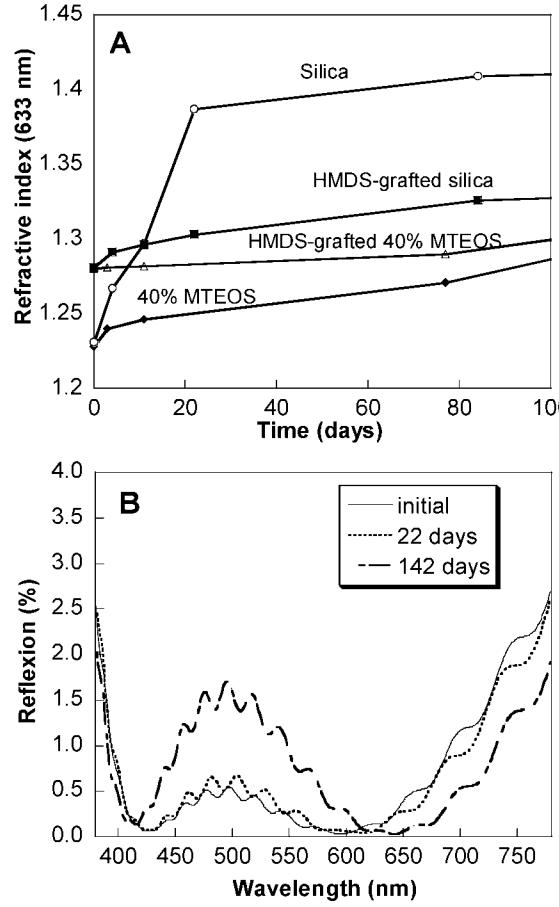

FIGURE 5. Graphs showing the stabilization of the organosilicate films toward water: (A) time evolution of the refractive index of different mesoporous calcined films stored in ambient atmosphere (RH = 40–60%); (B) reflectance spectrum of an interferential AR bilayer composed of a 40% MTES/TEOS mesoporous film ($n = 1.29$, 120 nm in thickness) and a high-index layer ($n = 1.75$, 140 nm in thickness) deposited on a polymer substrate.

The presence of methyl groups, introduced either by HMDS grafting or by two-step synthesis or both, hinders water adsorption and clearly improves the stability of films (Figure 5A). However, the refractive index of hybrid films is not completely stabilized in agreement with infrared spectra, which reveal that they are still able to adsorb organic pollutants. An HMDS–40% MTES/TEOS mesoporous film prepared by CTAB extraction with acetone was tested as the low-index layer in an interferential AR multilayer. The mesoporous film ($n = 1.29$, 120 nm in thickness) was deposited on a high-index layer ($n = 1.75$, 140 nm in thickness) deposited on a polycarbonate substrate. The reflectance spectrum of the interferential bilayer presents the expected W-shape with a value smaller than 0.5% in the major part of the visible range (Figure 5B). The AR treatment is stable after 21 days, but the average reflectance coefficient increases from 0.32% up to 1.5% after 4 months due to the increase of the index of the mesoporous layer (from 1.29 to 1.33). This confirms that more work is required to completely stabilize mesoporous films toward organic contaminations using hydrophobic and oleophobic organic groups.

Mesoporous Silica as Binders of TiO_2 Nanoparticles in Photocatalytic Films

The extraordinary properties of TiO_2 semiconductors in heterogeneous photocatalysis are now well-known, and their applications are widely investigated in many fields such as water splitting, photoelectrochemical cells, decontamination, or self-cleaning materials.[34,35] These two latter applications use the remarkable ability of TiO_2 pigments to degrade almost any organic molecule under UV light irradiation.[36] The mechanism of this phenomena has been the subject of numerous investigations.[37,38] As a rough description, absorption of UV photons leads to the generation of electron–hole pairs, a fraction of which are rapidly trapped at the surface of the oxide. The charges may react with adsorbed hydroxyls or oxygen molecules, yielding radicals, which then react very efficiently with the surrounding organic molecules, leading to volatile degradation byproducts or entire mineralization into CO_2, H_2O, and mineral acids.

In the special case of self-cleaning applications, for example, on glass windows, TiO_2 is deposited on the surface as a thin film of a few tens of nanometers to a few micrometers thickness.[39] The basic idea relies on the removal of pollutants by the action of the UV fraction of the sunlight.[40] In addition to the photocatalytic processes and in the case of outdoor applications, the hydrophilic properties of the TiO_2 allow the removal of dust or inorganic degradation byproducts by rain.

The TiO_2 thin films may be deposited using different methods such as sputtering,[41] chemical vapor deposition (CVD),[42] or sol–gel.[43] The sol–gel method consists of the deposition of the films from a liquid solution containing either colloidal TiO_2 nanoparticles[38,44] or TiO_2 molecular precursors that can be converted into nanocrystalline TiO_2 after a thermal treatment.[45,46] In all cases, the relatively soft conditions that are used lead to porous films with poor mechanical properties, recognized as a significant limitation for many practical applications of the sol–gel process. Nevertheless, many efforts are still devoted to the improvement of the sol–gel films, since the process is quite versatile, does not require costly equipment, and can be achieved on substrates with complex shapes. One way is to add in the formulation a compound that can act as a binder to improve the cohesion between the TiO_2 crystallites. Silica is often chosen for that purpose due to its remarkable ability to be processed by sol–gel chemistry as a polymeric network. Nevertheless, the presence of a binder should not hinder the diffusion pathways between the organic species to be degraded and the radicals generated at the surface of the oxide. It then appears quite clear that the optimization of sol–gel photocatalytic films should be performed through a good compromise between a high porosity and sufficiently good mechanical properties, and in addition with a controlled microstructure of the TiO_2 itself.

As an original development of our work on mesoporous silica films, we investigate a method of elaboration of photocatalytic TiO_2/SiO_2 coatings that allows a separate control of the film porosity and the TiO_2 microstructure. The basic principle of the film synthesis relies on the use of mesoporous silica as a binder for TiO_2 nanoparticles homogeneously dispersed within all the film thickness.[47] The use of mesoporous silica for the elaboration of photocatalytic materials has been described in several previous studies.[48] In most cases, the TiO_2 particles are formed in situ within the porous matrix after impregnation with a solution of precursors. Nevertheless, it was shown that the TiO_2 loading is quite low and the crystallinity of the TiO_2 crystallites is strongly limited by the low temperature of calcination imposed by the use of glass substrates (typically less than 450 °C). Here another approach is investigated consisting of using preformed TiO_2 particles, obtained through colloid chemistry routes, which are further redispersed inside surfactant-templated mesoporous silica films with a controlled porosity.

The synthesis process was directly adapted from our previous work on the elaboration of mesoporous silica films using a poly(ethylene oxide)/poly(propylene oxide) triblock copolymer (PE6800) as the surfactant.[47] The films obtained with a copolymer/Si ratio of 0.01 have been characterized and exhibit a total pore volume fraction of about 38%, distributed both as micropores (i.e., pores with diameter of a few angstroms) and mesopores (size of 5–6 nm) that are arranged with a textured face-centered orthorhombic structure.[49] TiO_2 nanoparticles are incorporable by the simple addition of a colloidal dispersion of well-crystallized anatase particles (Millennium S5-300) into the sol prior to its deposition. The individual particles consist of 50 nm aggregates of primary 7 nm anatase crystallites.

The good dispersion state of the particles is preserved after their addition into the silica sol containing the copolymer surfactant for Ti/(Ti + Si) molar ratios up to 0.8, and the obtained films are perfectly transparent. Rapid flocculation is however observed when the particles are added to the sol without the surfactant, and this is true even for low Ti/(Ti + Si) ratio. This shows that the copolymer ensures a steric stabilization of the particles through its interactions with their surface. Figure 6A shows a TEM picture of a representative film. The particles are well dispersed within all the film thickness and the organized porous structure, observed in pure silica films[49] (i.e., with no TiO_2), appears to be preserved between the particles.

The photocatalytic activity of the films was measured by monitoring the degradation of stearic acid deposited on the film under UV-A irradiation (Figure 6B). The degradation kinetics is deduced from the plot of the time evolution of the 2923 cm^{-1} band intensity from the CH_2 groups.[50,51] The kinetics is found to follow a first-order law over all the degradation curve, with a calculated rate constant k_1 that is typically equal to 0.09 min^{-1} for a sample with a Ti/(Ti + Si) molar ration of 0.5. It must be noted nevertheless that the degradation kinetics exhibit a more complex behavior than a simple one order rate, since the k_1 values calculated for different experiments

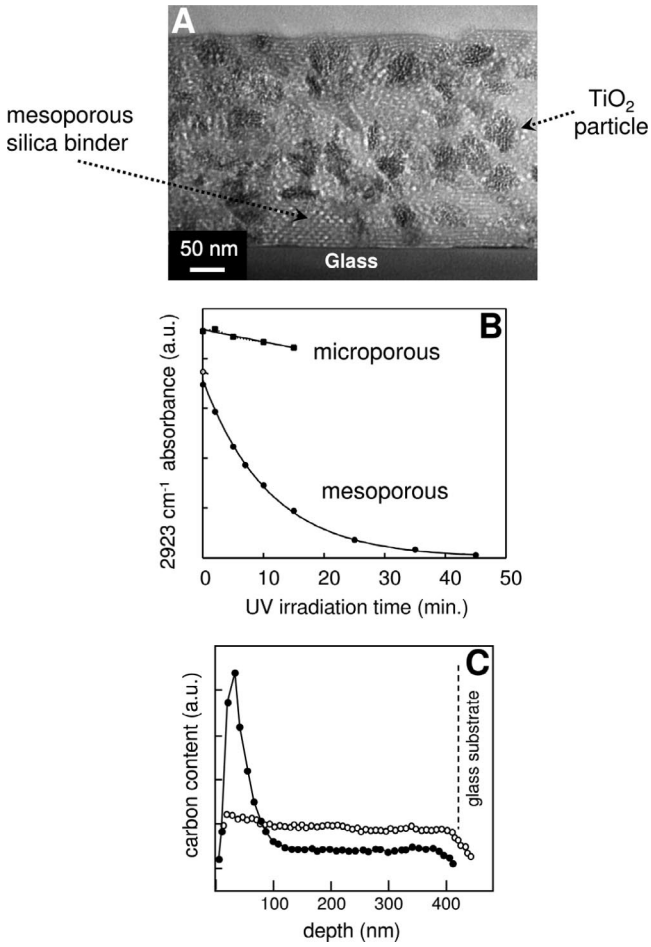

FIGURE 6. (A) Transmission electron microscopy image (transverse section) of a typical mesoporous silica/TiO_2 particles film obtained with Ti/(Ti + Si) = 0.2, (B) degradation curves of the stearic acid deposited on mesoporous (dots) and microporous films (squares), monitored through the evolution of the 2923 cm^{-1} vibration band from the CH_2 groups, and (C) SIMS profile of the carbon content for a microporous (bold) and a mesoporous film (plain) on which the stearic acid was deposited.

were found to decrease drastically when increasing the initial stearic acid concentration.[47]

For comparison, the degradation kinetics was also measured in the case of a film with a microporous binder, that is, obtained in the same way as the mesoporous one and with the same TiO_2 amount but without using the mesopore templating copolymer (Figure 6B). These films have a total pore volume fraction of about 16% with an average pore diameter of 2 nm.[47] First-order kinetics analysis of this sample activity gives a value of $k_1 = 0.006$ min^{-1}, which is less by a factor of about 15 than what was found in the case of the microporous film. This gives clear evidence of the influence of the film porosity on its degradation efficiency, independent of the microstructure of the TiO_2 crystallites. It can be reasonably assumed that the beneficial effect of the porosity may be mostly explained by an improved diffusion of the radicals or a closer proximity between the surface of the TiO_2 crystallites and the organic molecules to be degraded. This latter effect was confirmed by secondary ion mass spectrometry (SIMS) profiles of the carbon content just after deposition of stearic acid (Figure 6C). In the case of the mesoporous TiO_2 films, the organic molecules lie at the surface of the film, whereas they are found over all the film thickness in the case of the microporous one. This may explain the difference of degradation kinetics in two different ways: first, the average distance between the organic molecules and the surface of the TiO_2 crystallites is much lower in the case of the mesoporous materials, so that oxidizing radicals may react much more efficiently.[52] Second, stearic acid deposited on microporous or dense films forms a layer of significant thickness (about 17 nm in our experimental conditions), which may slow down the diffusion of oxygen or water molecules that are also involved in the degradation process.[44]

Concluding Remarks

For light emission, thin films made from stable luminescent inorganic nanoparticles clearly appear as an alternative to the existing white light emitters such as organic light-emitting diodes, polymer light-emitting diodes, and incandescent light bulbs. A crucial challenge for the chemist is both to develop efficient blue phosphors and to shift the excitation wavelength of particles toward the infrared range. This could be obtained by developing new systems able to emit visible light by the up-conversion process, that is, by near-infrared light excitation. Luminescent inorganic molecular clusters can also be considered as promising photoactive species for a large range of optical applications since they usually combine the photostability of the inorganic nanoparticles with the monodispersity of the organic molecules.

Although the use of mesoporous organized silica coatings as stable low-index layers still requires the improvement of their chemical stability, it can be noted that these coatings are very promising for future sol–gel applications in optics. First, their development is a confirmation that the sol–gel approach permits microstructural as well as compositional tailoring, which is not possible by other coating techniques such as sputtering, evaporation, or CVD. Second, they open the way to the preparation of multifunctional coatings as clearly shown by their role in TiO_2-photocatalytic devices in which their structural (porosity), chemical (hydrophilic character), and mechanical functions are used to optimize the catalytic efficiency.

The authors gratefully acknowledge Arnaud Huignard, Valérie Buissette, Sophie Besson, Muriel Matheron, and Emmanuelle Allain for their crucial contributions to the work discussed here. This work was supported by Rhodia, Essilor International, and Saint-Gobain.

References

(1) Brinker, C. J.; Scherer, G. W. *Sol-Gel Science*; Academic Press: London, 1990.
(2) Sanchez, C.; Lebeau, B.; Chaput, F.; Boilot, J-P. Optical properties of functional hybrid organic-inorganic nanocomposites. *Adv. Mater.* **2003**, *15* (23), 1969–1994.
(3) Service, R. F. Organic LEDs look forward to a bright, white future. *Science* **2005**, *310*, 1762–1763.

(4) (a) Shchekin, O. B.; Epler, J. E.; Trottier, T. A.; Margalith, T.; Steigerward, D. O.; Holcomb, M. O.; Martin, P. S.; Krames, M. R. High performance thin-film filp-chip InGaN-GaN light emitting diodes. *Appl. Phys. Lett.* **2006**, *89*, 071109. (b) Mueller, A. H.; Petruska, M. A.; Achermann, M.; Werder, D. J.; Akhadov, E. A.; Koleske, D. D.; Hoffbauer, M. A.; Klimov, V. I. Multicolor light-emitting diodes based on semiconductor nanocrystals encapsulated in GaN injection layer. *Nano Lett.* **2005**, *5* (6), 1039.

(5) Bai, G. R.; Zhang, H.; Foster, C. M. Preparation of YVO_4 thin films by metal organic chemical vapour deposition. *Thin Solid Films* **1998**, *321*, 115–122.

(6) Hao, J.; Studenikin, S. A.; Cocivera, M. Blue, green and red cathodoluminescence of Y_2O_3 phosphor films prepared by spray pyrolysis. *J. Lumin.* **2001**, *93*, 313–319.

(7) Korzenski, M. B.; Lecoeur, P.; Mercey, B.; Raveau, B. Nd:YVO_4 thin films grown by pulsed laser deposition: Effects of temperature and pressure on the grain morphology and microstructure. *Chem. Mater.* **2001**, *13*, 1545–1551.

(8) Pons-y-Moll, O.; Perriere, J.; Millon, E.; Defourneau, R. M.; Defourneau, D.; Vincent, B.; Essahlaoui, A.; Boudrioua, A.; Seiler, W. Structural and optical properties of rare-earth-doped Y_2O_3 waveguides grown by pulsed-laser deposition. *J. Appl. Phys.* **2002**, *92* (9), 4885–4890.

(9) Ravichandran, D.; Roy, R.; Chakhovskoi, A. G.; Hunt, C. E.; White, W. B.; Erdei, S. Fabrication of $Y_3Al_5O_{12}$:Eu thin films and powers for FED applications. *J. Lumin.* **1997**, *71*, 291–297.

(10) Rao, R. P. Growth and characterization of Y_2O_3:Eu^{3+} phosphor films by sol-gel process. *Solid State Commun.* **1996**, *99* (6), 439–443.

(11) Yu, M.; Lin, J.; Wang, Z.; Fu, J.; Wang, S.; Zhang, H. J.; Han, Y. C. Fabrication, patterning and optical properties of nanocrystalline YVO_4:A (A = Au, Dy, Sm, Er) phosphor films via sol-gel soft lithography. *Chem. Mater.* **2002**, *14* (5), 2224–2231.

(12) Yu, M.; Lin, J.; Fu, J.; Han, Y. C. Sol-gel fabrication, patterning and photoluminescent properties of $LaPO_4$:Ce,Tb thin films. *Chem. Phys. Lett.* **2003**, *37*, 178–183.

(13) Colvin, V. L.; Schlamp, M. C.; Alivisatos, A. P. Light-emitting diode made from cadmium selenide nanocrystals and semiconducting polymer. *Nature* **1994**, *370* (6488), 354–357.

(14) Klimov, V. I.; Mikhailovsky, A. A.; Xu, S.; Holligsworth, J. A.; Leatherdale, C. A.; Eisler, H. J.; Bawendi, M. G. Optical gain and stimulated emission in nanocrystal quantum dots. *Science* **2000**, *290* (5490), 314–317.

(15) Murray, C. B.; Kagan, C. R.; Bawendi, M. G. Synthesis and characterization of monodisperse nanocrystals and close-packed nanocrystals assemblies. *Annu. Rev. Mater. Sci.* **2000**, *30*, 545–610.

(16) (a) Riwotzki, K.; Haase, M. Wet-chemical synthesis of doped colloidal nanoparticles: YVO_4:Ln (Ln = Eu, Sm, Dy). *J. Phys. Chem. B* **1998**, *102* (50), 10129–10135. (b) Meyssamy, H.; Riwotzki, K.; Kornowski, A.; Naused, S.; Haase, M. Wet-chemical synthesis of doped colloidal nanomaterials: Particles and fibers of $LaPO_4$: Eu, $LaPO_4$:Ce, and $LaPO_4$:Ce,Tb. *Adv. Mater.* **1999**, *11* (10), 840–844.

(17) (a) Huignard, A.; Gacoin, T.; Boilot, J. P. Synthesis and luminescence properties of colloidal YVO_4:Eu phosphors. *Chem. Mater.* **2000**, *12* (4), 1090–1094. (b) Huignard, A.; Buissette, V.; Laurent, G.; Gacoin, T.; Boilot, J. P. Synthesis and characterizations of YVO_4:Eu colloids. *Chem. Mater.* **2002**, *14* (5), 2264–2269. (c) Buissette, V.; Moreau, M.; Gacoin, T.; Boilot, J. P. Colloidal synthesis of luminescent rhabdophane $LaPO_4$:Ln^{3+}-xH_2O (Ln=Ce, Tb, Eu; $x \approx 0.7$) nanocrystals. *Chem. Mater.* **2004**, *16* (19), 3767–3773.

(18) Buissette, V.; Moreau, M.; Gacoin, T.; Boilot, J. P. Luminescent core/shell nanoparticles with a rabdophane $LnPO_4$-xH_2O structure: Stabilization of Ce^{3+}-doped compositions. *Adv. Funct. Mater.* **2006**, *16*, 351–355.

(19) Buissette, V.; Giaume, D.; Gacoin, T.; Boilot, J. P. Aqueous routes to lanthanide-doped oxide nanophosphors. *J. Mater. Chem.* **2006**, *16*, 529–539.

(20) Wang, Y.; Tang, Z. Y.; Correa-Duarte, M. A.; Liz-Marzan, L. M.; Kotov, N. A. Multicolor luminescence by photoactivation of semiconductor nanoparticles films. *J. Am. Chem. Soc.* **2003**, *125*, 2830–2831.

(21) Schuetz, P.; Caruso, F. Electrostatically assembled fluorescent thin films of rare-earth-doped lanthanum phosphate nanoparticles. *Chem. Mater.* **2002**, *14*, 4509–4516.

(22) Huignard, A.; Gacoin, T.; Chaput, F.; Boilot, J. P.; Aschehoug, P.; Viana, B. Synthesis and luminescence properties of colloidal lanthanide doped YVO_4. *Mater. Res. Soc. Symp. Proc.* **2001**, 667.

(23) Huignard, A.; Buissette, V.; Franville, A.-C.; Gacoin, T.; Boilot, J. P. Emission processes in YVO_4:Eu nanoparticles. *J. Phys. Chem. B* **2003**, *107*, 6754–6759.

(24) Pettit, R. B.; Ashley, C. S.; Reed, S. T.; Brinker, C. J. Antireflective films from the sol-gel process. In *Sol-gel Technology for thin films, fibers, performs, electronics and specialty shapes*; Klein, L. C., Ed.; Noyes publications: Park Ridge, NJ, 1988; Vol. *5*, pp 80–109.

(25) Nostell, P.; Roos, A.; Karlsoon, B. Optical and mechanical properties of sol-gel antireflective films for solar energy applications. *Thin Solid Films* **1999**, *351*, 170–175.

(26) Chen, D. Anti-reflection (AR) coatings made by sol-gel process: A review. *Sol. Energy Mater. Sol. Cells* **2001**, *68*, 313–316.

(27) Bautista, M. C.; Morales, A. Silica antireflective films on glass produced by the sol-gel method. *Sol. Energy Mater. Sol. Cells* **2003**, *80*, 217–225.

(28) (a) Lu, Y.; Gangull, R.; Drewlen, C. A.; Anderson, M. T.; Brinker, C. J.; Gong, W.; Guo, Y.; Soyez, H.; Dunn, B.; Huang, M. H.; Zink, J. I. Continuous formation of supported cubic and hexagonal mesoporous films by sol-gel dip-coating. *Nature* **1997**, *389*, 364–368. (b) Besson, S.; Gacoin, T.; Ricolleau, C.; Jacquiod, C.; Boilot, J-P. Phase diagram for mesoporous CTAB-silica films prepared under dynamic conditions. *J. Mater. Chem.* **2003**, *13*, 404–409. (c) Grosso, D.; Cagnol, F.; Soler-Illia, A. A.; Crepaldi, E. L.; Amenitsch, H.; Brunet-Bruneau, A.; Bourgeois, A.; Sanchez, C. Fundamental of mesostructuring through evaporation-induced self assembly. *Adv. Funct. Mater.* **2004**, *14*, 309–322.

(29) Bruinsma, P. J.; Hess, N. J.; Bontha, J. R.; Liu, J.; Baskaran, S. Low-k mesoporous silica films through template-based processing. *Mater. Res. Soc. Symp. Proc.* **1997**, *443*, 105–110.

(30) Balkenende, A. R.; De Theije, F. K.; Kriege, J. C. K. Controlling dielectric and optical properties of ordered mesoporous organosilicate films. *Adv. Mater.* **2003**, *15* (2), 139–143.

(31) Grosso, D.; Balkenende, A. R.; Albouy, P-A.; Lavergne, M.; Mazerolles, L.; Babonneau, F. Highly oriented 3D-hexagonal silica thin films produced with cetyltrimethylammonium bromide. *J. Mater. Chem.* **2000**, *10*, 2085–2089.

(32) Matheron, M.; Bourgeois, A.; Gacoin, T.; Brunet-Bruneau, A.; Albouy, P-A.; Boilot, J-P.; Biteau, J.; Lacan, P. Mesoporous 3D-hexagonal organosilicate films: Post-synthesis grafting vs. Direct synthesis. *Thin Solid Films* **2006**, *495*, 175–179.

(33) Matheron, M.; Bourgeois, A.; Brunet-Bruneau, A.; Albouy, P-A.; Biteau, J.; Gacoin, T.; Boilot, J-P. Highly ordered CTAB-templated organosilicate films. *J. Mater. Chem.* **2005**, *15*, 4741–4745.

(34) Mills, A.; Le Hunte, S. An overview of semiconductor photocatalysis. *J. Photochem. Photobiol., A* **1997**, *108*, 1–35.

(35) Fujishima, A.; Rao, T. N.; Tryk, D. J. TiO_2 Photocatalysts and diamond electrodes. *Photochem. Photobiol., C* **2000**, *1*, 1–21.

(36) Pruden, A. L.; Ollis, D. F. Photoassisted heterogeneous catalysis–the degradation of trichloroethylene in water. *J. Catal.* **1983**, *82*, 404–417.

(37) Minabe, T.; Tryk, D. A.; Sawunyama, P.; Kikuchi, Y.; Hashimoto, K.; Fujishima, A. TiO_2-mediated photodegradation of liquid and solid organic compounds. *J. Photochem. Photobiol., A* **2000**, *137*, 53–62.

(38) Puzenat, E.; Pichat, P. Studying TiO_2 coatings on silica-covered glass by O_2 photosorption measurements and FTIR-ATR spectrometry–Correlation with the self-cleaning efficacy. *J. Photochem. Photobiol., A* **2003**, *160*, 127–133.

(39) Mills, A.; Hill, G.; Bhopal, S.; Parkin, I. P.; O'Neill, S. A. Thick titanium dioxide films for semiconductor photocatalysis. *J. Photochem. Photobiol., A* **2003**, *160*, 185–194.

(40) Paz, Y.; Luo, Z.; Rabenberg, L.; Heller, A. Photooxidative self-cleaning transparent titanium-dioxide films on glass. *J. Mater. Res.* **1995**, *10*, 2842–2848.

(41) DeLoach, J. D.; Scarel, G.; Aita, C. R. Correlation between titania film structure and near ultraviolet optical absorption. *J. Appl. Phys.* **1999**, *85*, 2377–2384.

(42) Mills, A.; Elliott, N.; Parkin, I. P.; O'Neill, S. A.; Clark, R. J. Novel TiO_2 CVD films for semiconductor photocatalysis. *J. Photochem. Photobiol. A: Chem.* **2002**, *151*, 171–179.

(43) Negishi, N.; Iyoda, T.; Hashimoto, K.; Fujishima, A. Preparation of transparent TiO_2 thin film photocatalyst and its photocatalytic activity. *Chem. Lett.* **1995**, *24* (9), 841–842.

(44) Vicente, J. P.; Gacoin, T.; Barboux, P.; Boilot, J-P.; Rondet, M.; Gueneau, L. Photocatalytic decomposition of fatty stains by TiO_2 thin films. *Int. J. Photoenergy* **2003**, *5*, 95–98.

(45) Watanabe, T.; Fukayama, S.; Miyauchi, M.; Fujishima, A.; Hashimoto, K. Photocatalytic activity and photo-induced wettability conversion of TiO2 thin film prepared by sol-gel process on a soda-lime glass. *J. Sol-Gel Sci. Technol.* **2000**, *19*, 71–76.

(46) Fretwell, R.; Douglas, P. An active, robust and transparent nanocrystalline anatase TiO_2 thin film–preparation, characterisation and the kinetics of photodegradation of model pollutants. *J. Photochem. Photobiol., A* **2001**, *143*, 229–240.

(47) Allain, E.; Besson, S.; Durand C.; Gacoin, T.; Boilot, J-P. Transparent Mesoporous Nanocomposite Films for Self-Cleaning Applications. *Adv. Funct. Mater.* **2006**, 10.1002/adfm.200600197.
(48) (a) Reddy, E. P.; Sun, B.; Smirniotis, P. G. Transition metal modified TiO2-loaded MCM-41 catalysts for visible- and UV-light driven photodegradation of aqueous organic pollutants. *J. Phys. Chem. B* **2004**, *108*, 17198–17205. (b) Lopez-Munoz, M-J.; van Griecken, R.; Aguado, J.; Marugan, J. Role of the support on the activity of silica-supported TiO_2 photocatalysts: Structure of the TiO2/SBA-15 photocatalysts. *Catal. Today* **2005**, *101*, 307–314.
(49) Besson, S.; Ricolleau, C.; Gacoin, T.; Jacquiod, C.; Boilot, J-P. Highly ordered orthorhombic mesoporous silica films. *Microporous Mesoporous Mater.* **2003**, *60*, 43–49.
(50) Sitkiewitz, S.; Heller, A. Photocatalytic oxidation of benzene and stearic acid on sol-gel derived TiO_2 thin films attached to glass. *New J. Chem.* **1996**, *20*, 233–241.
(51) Sawunyama, P.; Jiang, L.; Fujishima, A.; Hashimoto, K. Photodecomposition of a Langmuir-Blodgett film of stearic acid on TiO_2 film observed by in situ atomic force microscopy and FT-IR. *J. Phys. Chem. B* **1997**, *101*, 11000–11003.
(52) Lee, M. C.; Choi, W. Solid phase photocatalytic reaction on the soot/TiO_2 interface: The role of migrating OH radicals. *J. Phys. Chem. B* **2002**, *106*, 11818–11822.

AR600025J